



Glucose isomerisation into fructose over magnesium-impregnated NaY zeolite catalysts

I. Graça, D. Iruretagoyena, D. Chadwick*

Department of Chemical Engineering, Imperial College London, Exhibition Road, London SW7 2AZ, UK

ARTICLE INFO

Article history:

Received 13 October 2016

Received in revised form 2 January 2017

Accepted 14 January 2017

Available online 17 January 2017

Keywords:

Glucose

Fructose

Isomerisation

Zeolites

Magnesium

ABSTRACT

The performance of magnesium-impregnated NaY zeolite catalysts for the glucose isomerisation into fructose at 100 °C has been evaluated. Although crystallinity and textural properties of the zeolites are reduced through Mg addition, glucose conversion improves (6–49%) by increasing magnesium content (0–15 wt.%) due to an increase of the number of basic sites. Conversely, selectivity to fructose drops (96–66%). Nevertheless, good fructose yields were still reached with 10 and 15 wt.% of magnesium (about 32%), being similar or even higher than those found for a commercial hydrotalcite and a pure magnesium oxide. Catalysts lose performance through carbon retention and cations leaching. Deactivation of magnesium-based zeolites was further investigated by consecutive reaction runs. If no regeneration of the catalyst is performed, the activity of the zeolites decreases mainly as a result of cations leaching, the effect reducing with the number of runs. Regeneration allows the catalyst to recover almost totally its initial activity. Interestingly, used samples show higher fructose selectivity due to the additional pore opening resulting from cations leaching and/or carbon removal. Cations leaching results in a homogeneous catalytic reaction which is most significant for the highest magnesium content. Magnesium-based NaY zeolites are revealed as potential catalysts for glucose isomerisation into fructose with high fructose productivities and good performance in consecutive reactions combined with intermediate regeneration.

© 2017 Elsevier B.V. All rights reserved.

1. Introduction

Presently, most of the chemical industry is based on the use of fossil-derived resources. However, growing environmental concerns have increased pressure for their replacement by renewable resources. Biomass could be a promising alternative to fossil resources, as it is currently the only available renewable source of carbon able to be converted into fuels and value-added chemicals [1–3]. In particular, lignocellulosic biomass, i.e. agricultural, industrial and forest residues, has the advantage of being the cheapest and most abundant biomass type [1,4], and the only form of biomass that can grow without competition with food and in non-agricultural lands [1,5,6].

Lignocellulosic materials are composed of three different types of biopolymers, namely cellulose (glucose polymer), hemicellulose (shorter polymers of various sugars, principally xylose) and lignin (polymer of propyl-phenol), which after depolymerisation can be decomposed in their original monomers [1,3,7,8]. Cellulose is the major component of the lignocellulosic biomass, accounting for

about 40–80% of its structure [1,3,7], meaning that glucose is the most available biomass-derived monosaccharide. Glucose has been used as starting material in several industrial processes, mainly in the food industry and medicine [9–11]. However, glucose has also great potential to be applied in the synthesis of fuels, important platform chemicals, and polymeric materials, replacing the traditional petroleum-based feedstocks [1,3,12,13]. This has opened a wide range of possibilities for the valorisation of biomass-derived glucose.

In recent years, attention has been focused on the valorisation of biomass-derived glucose through isomerisation into fructose, as fructose is a key intermediate in the production of platform chemicals, such as 5-hydroxymethylfurfural (HMF), levulinic acid or lactic acid [14–17]. HMF, for instance, can be used in principle to produce caprolactam, the monomer for nylon-6 [18].

The isomerisation of glucose into fructose can be carried out using both biological and chemical catalysts, and mild conditions are normally applied. In the current industrial process, immobilised enzymes, D-glucose or xylose isomerase, are used as catalysts, with the maximum glucose conversion achievable being mainly governed by the thermodynamic equilibrium between both sugars, at the reaction temperature (usually 45–60 °C) [19–21]. Nevertheless, in spite of being one of the largest and most successful biocatalytic

* Corresponding author.

E-mail address: d.chadwick@imperial.ac.uk (D. Chadwick).

processes, it presents some disadvantages, such as high operating costs due to the irreversible deactivation of the enzymes and their periodic replacement, the need for an extremely pure glucose feedstock that implies the use of several pre-reaction purification steps and the rigorous control of the reaction conditions (temperature, pH, etc) to maximise enzymes lifetime [17,22]. This makes the use of enzymes less attractive in the context of biomass valorisation, giving rise to the need for a suitable chemical catalyst.

Homogeneous and heterogeneous catalysts have been investigated for the isomerisation of glucose to fructose [17]. Most studies of homogeneous catalysts have focused on soluble inorganic bases, such as sodium or potassium hydroxide, and organic bases, for example triethylamine [17,23–26]. Basic homogeneous catalysts, however, tend to form higher amounts of by-products [17,25]. Very few works have been so far carried out using Lewis-acid homogeneous catalysts, and only two salts have been tested, CrCl_3 and AlCl_3 [27]. Overall, both basic and acid homogeneous catalysts present good results for the glucose isomerisation into fructose, but they are corrosive and not as environmentally clean and cost-effective as solid catalysts, which can be much more easily separated from the products, regenerated and recycled to the process.

Heterogeneous catalysts tested for the isomerisation of glucose into fructose are mostly basic solid materials such as hydrotalcites [28–31], alkaline-exchanged zeolites [28,30,32], anion-exchanged resins [33], mesoporous ordered molecular sieves of the M41S family [34], magnesium oxide [35] and metallosilicate solid bases [36]. Temperatures below 120 °C are usually used in order to avoid secondary transformations, and water is commonly selected as solvent. In the case of magnesium oxide, high glucose conversions (62–67%) are reached after 1 h of reaction at 100 °C, which were even higher than the equilibrium glucose conversion at 100 °C (57% [21]), but with low fructose selectivities (38–44%) [35]. On the other hand, hydrotalcites, alkaline-exchanged zeolites and metallosilicates have demonstrated not only reasonable activity but also high selectivity to fructose (60–86%) under similar operating conditions [28–32,36].

Despite the good results, the use of zeolites for sugars isomerisation has been relatively scarce. Na-exchanged X, Y and A zeolites have been the most investigated basic materials [28,30,32]. In these studies, A and X zeolites present better performances for the sugars transformation than the Y zeolite, which appears to be mostly dependent on the Si/Al ratio, as the lower this parameter the greater the degree of ion-exchange with Na. Nevertheless, no major structural correlations have been established. Another tested property was the type of ion-exchanged cation, the monovalent cations (Li^+ , Na^+ , K^+ and Cs^+) being more active and selective than divalent cations (Ba^{2+} and Ca^{2+}). The activity increases from Li to Cs, but the selectivity to fructose was found to be higher using Na as compensating cation. The main noticed drawback was the compensating cations leaching from the zeolite framework to the liquid product during the reaction, leading to the catalyst deactivation.

More recently, it was found that zeolites with acidic properties, mainly Lewis acid sites, could also play a role in the isomerisation of glucose to fructose [17]. Indeed, Sn-Beta zeolite was reported to be particularly active for this reaction, when compared to other Sn-containing zeolites and mesoporous silica or to Ti-based catalysts, in either aqueous or acidic media [17,22,37,38]. Commercial acidic zeolites, such as H-Y, H-USY and H-beta, were as well successfully applied to the conversion of glucose to fructose in a two-step reaction procedure, using methanol and water as solvents [39]. H-USY ($\text{Si}/\text{Al} = 6$) zeolite was demonstrated to be the most active, yielding 55% of fructose after 1 h of reaction at 120 °C, which could be mainly due to the larger pore size and the presence of extra-framework aluminium species (EFAL).

Therefore, either basic or acid zeolite-based materials are promising catalysts for the glucose isomerisation into fructose.

However, their potential to perform this reaction has not been fully explored to date, especially considering the versatility of zeolites. In this respect, the influence of added divalent cation species to basic zeolites remains a relatively unstudied area. In this work, the effect of magnesium impregnation of NaY zeolite on the performance for glucose isomerisation into fructose has been investigated at 100 °C in aqueous medium. NaY zeolite was selected as support, since it is a large pore zeolite allowing an easier diffusion of the bulky glucose molecules to the interior of its pore system [40], and it presents framework basicity given by the Na-exchange [28]. The attraction of magnesium as dopant lies in the expected formation of MgO in the zeolite pore structure, since MgO has high intrinsic basicity [41]. It is also environmentally relatively benign when compared to other promoters, for instance Sn. The influence of magnesium content on the activity and selectivity of the zeolites, as well as the effect of the reaction time, have been analysed. This paper also addresses the study of the catalyst deactivation and ability to be reutilised in sequential runs, with and without an intermediate regeneration step. The prepared catalysts were characterised by X-Ray diffraction (XRD), N_2 adsorption, transmission electron microscopy (TEM) and temperature programmed desorption of CO_2 (CO_2 -TPD), and their properties correlated to the catalytic activity. We show that the addition of Mg leads to promising catalysts with fructose yields and productivities approaching or even exceeding previously reported values.

2. Experimental

2.1. Catalyst preparation

A commercial NaY zeolite supplied by Zeolyst (CBV 100), with unit cell formula $\text{Na}_{34}\text{H}_4\text{Al}_{38}\text{Si}_{139}\text{O}_{384}\text{15EFAL}$, was used as support. Global Si/Al ratio (2.6) was given by supplier and framework Si/Al ratio (3.6) was calculated from the unit cell parameter ($a_0 = 2.455 \text{ nm}$) using the Breck-Flanigen equation. Samples with different Mg contents (5–15 wt.%) were prepared by incipient wetness impregnation of the NaY zeolite, using magnesium nitrate hexahydrate ($\text{Mg}(\text{NO}_3)_2 \cdot 6\text{H}_2\text{O}$, Sigma-Aldrich, 99% purity) as precursor salt. Prior to the impregnation, the zeolite was dried in an oven at 100 °C. An aqueous solution of the Mg salt with a water volume close to that of the zeolite pores was then added drop-wise to the zeolite, while stirring. After that, samples were dried in an oven overnight at 100 °C, and, finally, calcined at 500 °C under air flow. The samples are identified as 5%MgNaY, 10%MgNaY and 15%MgNaY.

A commercial MgO provided by Sigma-Aldrich with 97% purity, a commercial hydrotalcite with nominal 3:1 Mg/Al ratio (Sigma-Aldrich), as well as a mechanical mixture of NaY zeolite and MgO (10 wt.%), which was prepared by mixing in a mortar the required amount of both materials until complete homogenisation of the sample, were also used as catalysts for comparative purposes.

2.2. Catalyst characterisation

Powder XRD patterns were obtained in a PANalytical X'Pert Pro diffractometer, using $\text{Cu K}\alpha$ radiation and operating at 40 kV and 40 mA. The scanning range was set from 5° to 80° (2θ), with a step size of 0.0017°/s.

N_2 adsorption measurements were carried out at –196 °C on a Micrometrics 3Flex apparatus. Before adsorption, zeolite samples were degassed under vacuum at 90 °C for 1 h and then at 350 °C overnight. The total pore volume (V_{total}) was calculated from the adsorbed volume of nitrogen for a relative pressure P/P_0 of 0.97, whereas the micropore volume (V_{micro}) and the external surface

area (S_{ext}) were determined using the t-plot method. The mesopore volume (V_{meso}) was given by the difference $V_{total} - V_{micro}$.

Transmission electron microscopy (TEM) was performed by using a JEOL2010 Transmission Electron Microscope operating at 200 kV. The samples were prepared by dispersing a small amount of solid in ethanol and allowing a drop contacting with a copper grid coated with holey carbon film and the ethanol evaporating.

Temperature programmed desorption (TPD) of CO₂ was carried out using a quartz micro-flow-column system operated at atmospheric pressure. The sample (100 mg) was pre-conditioned by heating from room temperature to 400 °C at 10 °C/min by flowing 100 mL/min of Ar. After cooling to 50 °C, the sample was exposed to a 20% CO₂/Ar premixed gas (BOC) for 1 h. The system was then purged in flowing Ar for 1 h to remove physisorbed CO₂, and the temperature was then increased to 700 °C at 50 °C/min. A mass spectrometer (ESS GeneSys II with capillary sample line) was used to monitor the CO₂ concentration in the quartz tube exit gas stream. The TPD response was calibrated injecting 2 mL of the premixed CO₂ gas.

Spent catalysts were analysed for the carbonaceous materials deposition after reaction using thermogravimetric analysis (TGA), which was carried out in a TA Instruments TGA Q500. The samples were heated up from room temperature to 900 °C, at 10 °C/min, under air flow (60 mL/min). The weight loss was recorded as a function of the temperature.

2.3. Catalytic test

Glucose isomerisation reaction was performed in a 25 mL Büchi AG autoclave at 100 °C, under inert atmosphere. An initial nitrogen pressure of 3 bar was used in order to avoid air entering the system. Before the reaction, a solution containing 0.5 g of D-glucose (Sigma, ≥99.5% purity) in 5 mL of deionised water was prepared and fed to the reactor, which already contained the catalyst. An identical amount of catalyst was used in each run (100 mg). The reactor was sealed, purged with nitrogen and the initial working pressure was set. An oil bath was used to heat up the reactor to the desired temperature. The reaction was carried out for 0.5, 1, 2 or 3 h, under continuous stirring (1000 rpm) to have a well-mixed condition and avoid external diffusional limitations. After the reaction,

the reactor was cooled down, the nitrogen was released and the liquid product-catalyst suspension collected. A reaction run starting from D-fructose (Sigma, ≥99% purity) was also accomplished.

In order to analyse the reaction effluent, the catalyst was firstly separated from the mixtures by centrifugation at 5000 rpm for 5 min. All the liquid samples were diluted in water and analysed by high-performance liquid chromatography (HPLC), using a Shimadzu Prominence UFLC system equipped with refractive index (RID-10A) and UV-210 nm (SPD-20A) detectors. The analysis was carried out with a Supelcogel™ C-610H HPLC column, thermostated at 30 °C. The mobile phase was a 0.1% (v/v) H₃PO₄ aqueous solution at a flow rate of 0.3 mL/min. Citric acid was added as standard. The experimental errors in the conversion and yield are on average 2% and in the selectivity 7%.

Leaching of cations from the catalysts to the reaction mixture was analysed by inductively coupled plasma (ICP), using a PerkinElmer Optima 2000 DV ICP system.

Total organic carbon content in the liquid product was determined using a Sievers InnovOx Laboratory TOC analyser provided by GE Instruments.

3. Results and discussion

3.1. Catalyst characterisation

Powder XRD diffractograms obtained for the different prepared zeolites are presented in Fig. 1. First of all, it can be seen that all the zeolites present the characteristic peaks of the FAU structure [42]. However, the results show a progressive decrease of the intensity of the diffraction peaks in comparison to the pure NaY zeolite. This can be related simply to the decreasing proportion of zeolite in the sample and/or to an actual reduction of the crystallinity of the zeolite structure due to the Mg addition. Based on the XRD patterns and having as reference the parent NaY, the crystallinities for the 5–15 wt.% Mg zeolites were determined to be 92, 77 and 75%, respectively. This suggests that in the samples containing higher amount of Mg there is some reduction of the intrinsic zeolite crystallinity. This partial damage of the zeolite structure could also be confirmed in TEM analysis. Fig. 2 shows the TEM micrographs obtained for the zeolites presenting 5 and 10 wt.% of magnesium

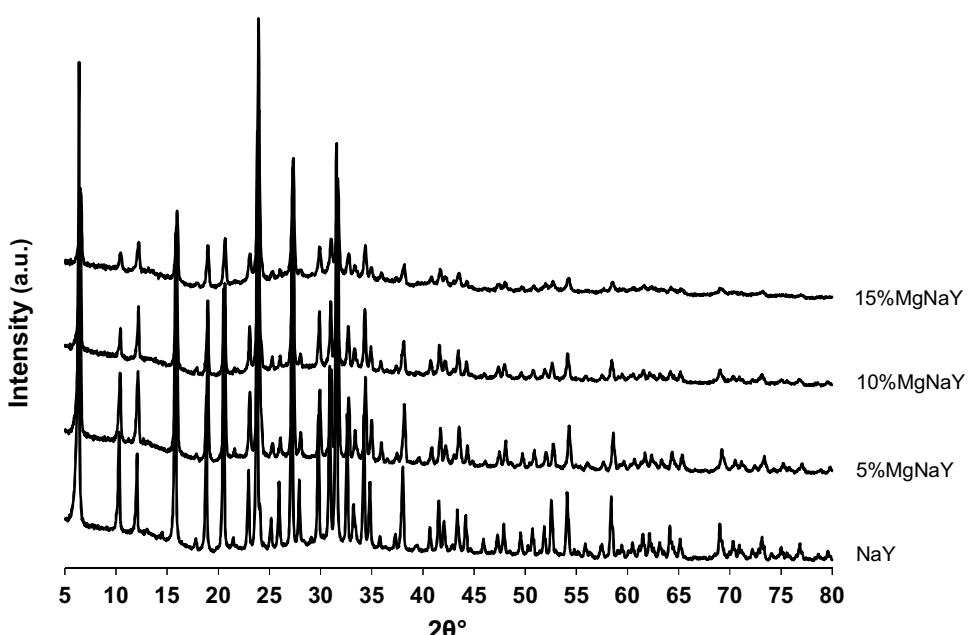


Fig. 1. XRD diffraction patterns for all the prepared zeolite samples.

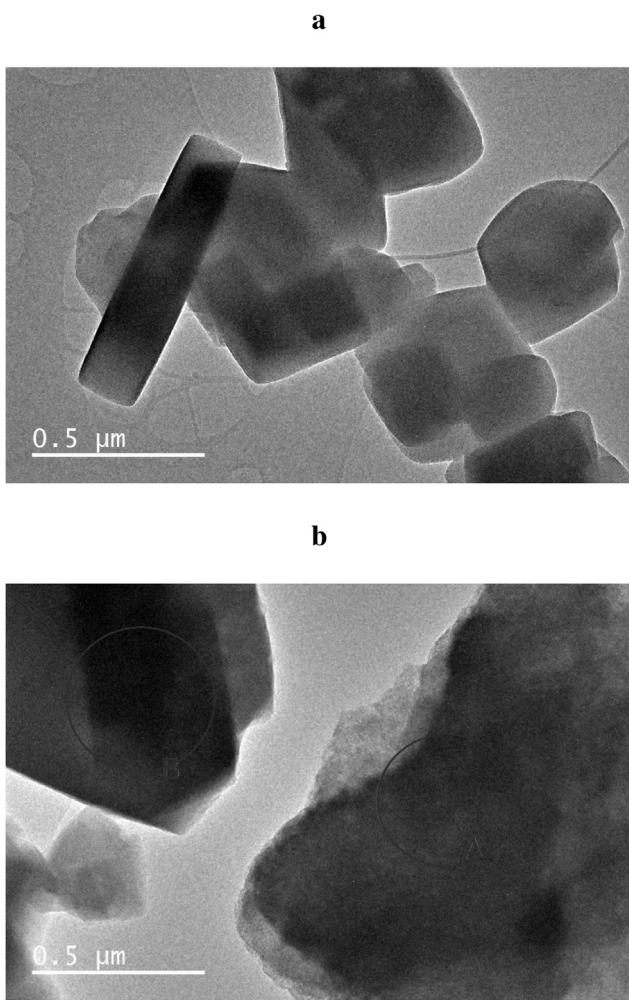


Fig. 2. TEM micrographs for the (a) 5%MgNaY and (b) 10%MgNaY zeolites.

in which the slight erosion of the zeolite crystals' edges at higher metal loadings is clearly visible.

XRD did not identify the presence of MgO ($2\theta = 37.0, 43.0, 62.4, 74.8$ and 78.7° [43,44]) on the calcined zeolite resulting from the NaY zeolite impregnation with the magnesium salt (Fig. 1). This could mean that the MgO entities might be small enough to escape the XRD detection (~ 3 nm) or that formed MgO is amorphous. No further conclusion on the size of any MgO particles can be made, as metal oxide entities could not be observed by TEM due to insufficient contrast between the elements in the zeolite framework and the metal oxide species (Fig. 2).

In order to investigate how the addition of magnesium affects the zeolite textural properties, microporous and mesoporous volumes and external surface areas of the zeolite catalysts were determined by nitrogen adsorption measurements. Data obtained for the magnesium-zeolites can be found in Table 1. Incorpora-

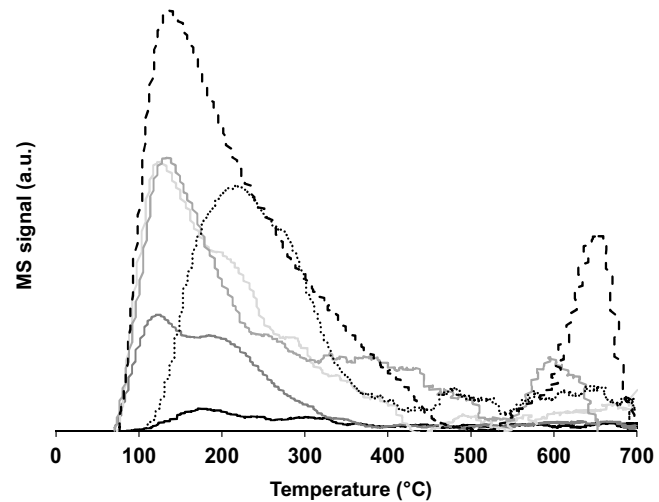


Fig. 3. CO_2 -TPD results for NaY (black line), 5%MgNaY (dark grey line), 10%MgNaY (medium grey line), 15%MgNaY (light grey line), MgO (dotted line) and commercial hydrotalcite (dashed line).

tion of magnesium on the zeolites at increasing amounts leads to a significant reduction of both the microporous and mesoporous volumes, when compared to the pure NaY zeolite. This decrease appears to be higher in the case of the mesopores. Indeed, when adding 15 wt.% of Mg to the NaY zeolite, a reduction of about 54% is observed for the microporous volume, whereas the mesoporous volume decreases by 72%. Conversely, only a small reduction is noticed in the external surface area due to the magnesium impregnation. Thus, the results seem to indicate that the magnesium species were preferentially associated with the mesoporosity of the zeolite. The presence of these magnesium entities on the mesopores could cause a partial blockage of the micropores of the zeolite or, additionally, some magnesium species could be as well inside the micropores.

Since this study aimed at the preparation of basic zeolite materials for the glucose isomerisation into fructose, the basicity of the catalysts was analysed by CO_2 -TPD (Fig. 3) [41,45]. Fig. 3 shows the CO_2 -TPD profiles for the pure NaY zeolites and the zeolites containing 5–15 wt.% Mg, where they are compared to the results found for the commercial hydrotalcite and the bulk MgO. Based on the CO_2 -TPD curves, CO_2 adsorption capacity was estimated for the zeolite samples (Table 1). Pure NaY zeolite presents a very low CO_2 adsorption capacity when compared to the other zeolites. CO_2 desorption for this catalyst mainly takes place between 100–350 °C, with maximum at about 200 °C, showing the weak basic character of the NaY zeolite in agreement with the literature data [46,47]. The basic sites density of the pure NaY zeolite is increased through Mg addition [48]. However, it can be seen that no further benefit is achieved by overloading the sample with magnesium, since no major differences in the CO_2 -TPD patterns can be observed when increasing the magnesium content from 10 to 15 wt.%. This could be due to an increase of the Mg species size or to the partial

Table 1
Textural properties and CO_2 adsorption capacity for the zeolite catalysts.

Catalyst	V_{micro} (cm^3/g)	V_{meso} (cm^3/g)	S_{ext} (m^2/g)	CO_2 ($\mu\text{mol/g}$)
NaY	0.317	0.247	51	26
5%MgNaY	0.205	0.130	41	101
10%MgNaY	0.192	0.194	40	231
15%MgNaY	0.145	0.070	45	260
5%MgNaY after 3 runs	0.266	0.159	80	–
5%MgNaY after 1 run with regeneration	0.273	0.176	106	–

V_{micro} = micropore volume; V_{meso} = mesopore volume; S_{ext} = external surface area.

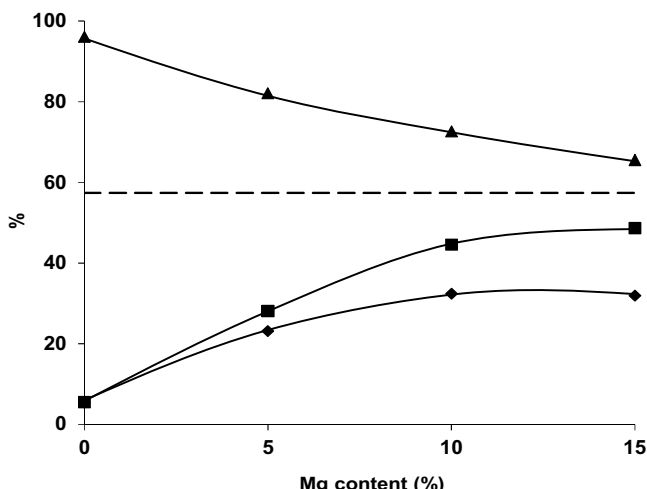


Fig. 4. Evolution of the glucose conversion (■), fructose yield (◆) and fructose selectivity (▲) as a function of the magnesium amount on the prepared zeolites, at 100 °C after 2 h. 0% of magnesium corresponds to the pure NaY zeolite. Glucose thermodynamic equilibrium conversion – dashed line.

pore blockage, leading to a decrease of the surface area for adsorption. In addition, generally, with the magnesium incorporation, two main CO₂ desorption bands maxima are noticed, one at around 130 °C and another at 200 °C corresponding to at least two different basicity strengths. According to the literature [49–51], the CO₂ desorption peak at lower temperature could be assigned to the CO₂ adsorption as bicarbonate species on MgO surface hydroxyl groups, whereas CO₂ desorption at higher temperatures is more commonly attributed to bidentate carbonates on Mg²⁺-O²⁻ pair sites and monodentate carbonates on isolated surface O²⁻ ions (low-coordination anions) present in the defects of the MgO surface. Moreover, Belin et al. [50] showed that bicarbonate species appear to be the dominant CO₂ adsorbed species on Mg-impregnated NaX zeolites. In addition, the calcination temperature is reported to influence the proportion of the various basic sites, weaker basic sites prevailing with an increase of the temperature due to a reduction of the MgO surface defects [51]. This is in agreement with the higher intensity of the band at 130 °C for the Mg-impregnated NaY zeolites of the present work. This indicates that the MgO species on the zeolites mainly present low basicity, which is smaller than the basicity (in density and strength of basic sites) of the pure MgO and the commercial hydrotalcite. Therefore, the addition of magnesium seems to mainly lead to an increase of the relatively weak basic sites density rather than promoting the basicity strength, when compared to the pure NaY zeolite.

3.2. Catalyst performance

All the prepared zeolite catalysts were tested for glucose isomerisation into fructose at the operating conditions described in 2.3 above. The influence on the activity, yield and selectivity of having increasing amounts of magnesium on the samples, the use of different reaction times, the identification of the main causes for the catalyst deactivation, as well as the behaviour of the catalysts after consecutive reaction runs with and without intermediate regeneration step, have been investigated. Comparisons between the prepared zeolite catalysts with reference catalysts including a commercial hydrotalcite and pure MgO and with literature data were also made.

3.2.1. Activity and selectivity of magnesium-impregnated zeolites

Fig. 4 shows the evolutions of the glucose conversion and the fructose yield and selectivity after 2 h of reaction as a function of

the magnesium content. Mannose was not detected in any significant amount in the liquid product for the Mg impregnated catalysts (Supplementary information, Figs. S1–S6). First, the support without any magnesium has only residual activity, the glucose conversion being 5.6%. However, the addition of magnesium clearly leads to a significant enhancement of the catalyst performance, which is consistent with the observed increase of the number of basic sites on the catalysts (Fig. 3). This improvement is mainly important when 5 wt.% of magnesium is impregnated, when the glucose conversion increased from 5.6% to 28.2% and the fructose yield from 5.4% to 23.1% compared to the support alone. The further promotion of the NaY zeolite with higher magnesium contents still leads to an enhancement of the catalyst performance, but to a lower extent. This is not surprising considering that there are contradictory effects influencing the catalyst performance. On one hand, greater amounts of magnesium increase the basicity of the sample (see Fig. 3), promoting the catalyst activity for glucose isomerisation into fructose, but with the increase of the magnesium amount the size of the MgO species could certainly be increased, lowering the activity. Moreover, as observed by XRD (Fig. 1) and TEM (Fig. 2), the crystallinity of the zeolites appears to be affected with increase of the magnesium content, which could also cause a detrimental effect on the activity by changing the metal oxide dispersion and interaction with the support. Besides this, the reaction rate can also slow down at higher magnesium content because of the approach to the thermodynamic equilibrium conversion for the glucose isomerisation to fructose at the studied temperature (57% [21]).

Furthermore, if one compares the results obtained for the catalysts containing 10 and 15 wt.% of magnesium, glucose conversions and fructose yields for both samples barely change. Therefore, it can be said that at 10–15 wt.% of magnesium the maximum performance of the catalyst for the reaction has been reached. As previously discussed (Fig. 3), the addition of a higher amount of magnesium does not contribute to an enhancement of the basicity of the material. Moreover, the greater reduction of the textural parameters for the zeolite with 15 wt.% of magnesium (Table 1) might as well have an impact on the catalyst performance, as it could prevent the bulky glucose molecules to penetrate the zeolite structure and/or limit the diffusion of the fructose molecules to the outside of the zeolite structure, leading to a higher carbonaceous materials accumulation in the zeolite structure. Higher reaction rates for the glucose isomerisation were also observed previously [39] for a USY zeolite presenting larger pore size when compared to other zeolites.

Another interesting observation concerns the fructose selectivity for these catalysts, which gradually decreases from 96.0 to 65.5% (glucose conversion from 5.6 to 48.7%) with the increase of the magnesium loading (Fig. 4). The evolution of the fructose yield (Fig. 4) indicates that the observed decrease of the selectivity is due to the further conversion of fructose. In fact, increasing the magnesium content from 10 to 15 wt.% Mg causes only a small increase of the glucose conversion from 44.6 to 48.7%, whereas the fructose yield (32%) remains unchanged. This means that the addition of magnesium is also leading to the formation of by-products. If one considers that fructose is forced to remain longer inside the zeolite structure because of partial blockage of the pores caused by the magnesium (Table 1), it will certainly undergo secondary transformations [52–54].

The possible contribution of homogenous phase reactions to the glucose isomerisation caused by the leaching of soluble species from the catalysts was assessed in the following way. The calcined 5–15 wt.% Mg catalysts were contacted with water at 100 °C for 2 h under nitrogen and stirring. The leached catalysts were separated from the liquid products by centrifugation and glucose was added to the recovered liquid phase and reacted at 100 °C for another 2 h.

Table 2

Sodium and magnesium leaching from the catalysts after contact with liquid water at 100 °C for 2 h, and homogeneous glucose conversions and fructose yields.

Catalyst	Na leaching % ^a (ppm) ^b	Mg leaching % ^a (ppm) ^b	Homogeneous glucose conversion (%)	Homogeneous fructose yield (%)
NaY	1.9 (36)	—	6.8	6.5
5%MgNaY	29.6 (571)	0.3 (3.4)	9.1	8.6
10%MgNaY	30.2 (582)	0.8 (7.9)	9.7	9.4
15%MgNaY	27.3 (527)	2.8 (28)	28.6	27.4

^a Percentage of leaching calculated by dividing the amount of Na or Mg removed from the zeolite during the run to the initial amount of Na (9.6 mg) or Mg (5, 10 or 15 mg) on the catalyst.

^b Concentration of Na or Mg in the liquid product (5 mL) after reaction.

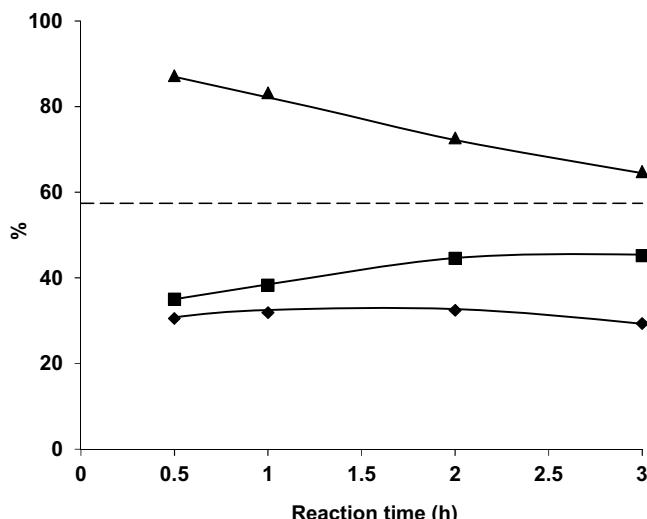


Fig. 5. Evolution of the glucose conversion (■), fructose yield (◆) and fructose selectivity (▲) as a function of the reaction time over the 10%MgNaY zeolite, at 100 °C. Glucose thermodynamic equilibrium conversion – dashed line.

Sodium and magnesium leaching after contact with water and the obtained homogeneous glucose conversions and fructose yields are given in Table 2. It appears that for the NaY support, the activity might derive mainly from the homogeneous reaction. For the 5–10 wt.% MgNaY zeolites, the homogeneous reaction could be associated mainly with the increased Na leaching from the impregnated catalysts (Table 2). The homogeneous catalytic contribution becomes more significant for the 15 wt.% Mg zeolite when the zeolite is probably overloaded with Mg. Thus, both homogeneous and heterogeneous catalytic reactions occur during the isomerisation of glucose into fructose over Mg-impregnated zeolite catalysts being mainly a heterogeneous reaction for low to medium Mg contents.

3.2.2. Effect of reaction time

Glucose isomerisation was also carried out at different reaction times, 0.5–3 h, over the 10%MgNaY zeolite (Fig. 5). First of all, it can be noticed that the evolution of the fructose yield with the reaction time passes through a maximum and then decreases, which is clear evidence that the by-products are produced from further transformation of fructose. This was also confirmed by running a reaction over the same catalyst using fructose as reactant. 44.0% fructose conversion was attained with the main by-products appearing to be the same as those found in the experiments starting from glucose. Glucose selectivity was only 21.3%.

Regarding glucose conversion vs. reaction time, the reaction rate seems to be very fast at shorter times, as the activity practically reaches a plateau after 0.5 h of reaction. In order to confirm that the glucose conversion achieved after 0.5 h was not a consequence of an adsorptive process, total organic carbon in the liquid product was analysed. An amount of 206.8 mg of carbon was determined, which matches the quantity of carbon initially in solution coming

from glucose (207.4 mg). Thus, this result clearly shows that the obtained conversion was reaction controlled over the first half hour. Identical results were found by Lecomte et al. [29] for a hydrotalcite and a KX zeolite. The glucose conversion still slightly increases from 0.5 to 2 h, but practically no improvement of the activity can be observed when 3 h of reaction are accomplished. Therefore, fructose selectivity drops with the increase of the reaction time. The observed stabilisation of the catalyst activity when runs longer than 2 h are performed might be due to the proximity to the thermodynamic equilibrium conversion for this reaction at 100 °C and/or to the greater catalyst deactivation at higher reaction times. The deactivation is investigated and discussed later in this paper. Overall, data presented in Fig. 5 show that maximum fructose productivity is achieved between 1 and 2 h of reaction.

3.2.3. Deactivation and regeneration of magnesium-impregnated zeolites

Possible causes leading to the deactivation of these catalysts after reaction were analysed in this work. Two main causes were identified: formation and retention of carbonaceous materials inside the zeolite structure (coke) and Na and Mg leaching from the zeolite to the liquid product. 3.6–9.6 wt.% of coke was found on the spent magnesium zeolites by thermogravimetric analysis (Table 3). Cations leaching was determined by ICP of the obtained liquid product solution; up to 50% of Na and 21% of Mg were lost from the magnesium zeolites to the liquid product as Mg content increased (Table 3). Both Na and Mg in solution increase with Mg content on the zeolites (see concentration in the liquid product in Table 3). While the percentages of Na removed from the low Mg zeolites in a normal reaction (Table 3) and a pre-leaching run (Table 2) are not very different, the quantity of Mg leached is much higher when glucose and the catalyst are both present in the reactor. This could be an indication that glucose and/or fructose are acting as chelating agents [55], favouring Mg removal from the catalyst. 12–30% of cation leaching (Li, Na, K, Cs) was also observed by Moreau et al. [28] during the same reaction over ion-exchanged A, X and Y zeolites. Such an important leaching of Na from the zeolites could indicate that Na is being replaced by H₃O⁺ as compensating cation due to the presence of water, reducing the basic nature of the zeolite. Indeed, hydronium exchange was proved to take place in all aqueous ion-exchanges involving zeolites [56–58]. Na might be as well substituted by Mg as this is also present in the reaction medium.

The effect of reaction time on the deactivation was studied for the 10%MgNaY zeolite, Table 3. There may be evidence of a slight increase of the magnesium leaching from the catalyst in the first hour of reaction. On the other hand, sodium leaching probably does not depend on the reaction time. Regarding coke retention on the zeolite, generally it slightly increases with reaction time.

In order to evaluate in more detail how deactivation affects the performance of these catalysts, consecutive catalytic tests were carried out over the 5%MgNaY zeolite, always under the same operating conditions (2 h, 100 °C). In the first set of experiments, three consecutive reaction runs were performed, the catalyst being reused without any regeneration. In between each run, the liquid

Table 3

Sodium and magnesium leaching and coke retention on the catalysts. Effect of reaction time given for the 10%MgNaY zeolite.

Catalyst	Reaction time (h)	Na leaching % ^a (ppm) ^b	Mg leaching % ^a (ppm) ^b	Coke (wt.%)
5%MgNaY	2	27.3 (527)	7.5 (75)	3.6
10%MgNaY	0.5	41.1 (794)	17.2 (344)	6.0
	1	39.1 (754)	21.0 (420)	6.7
	2	37.8 (730)	18.8 (376)	5.1
	3	34.3 (661)	22.2 (444)	9.6
15%MgNaY	2	49.9 (963)	21.0 (629)	8.3

^a Percentage of leaching calculated by dividing the amount of Na or Mg removed from the zeolite during the run to the initial amount of Na (9.6 mg) or Mg (5, 10 or 15 mg) on the catalyst.

^b Concentration of Na or Mg in the liquid product (5 mL) after reaction.

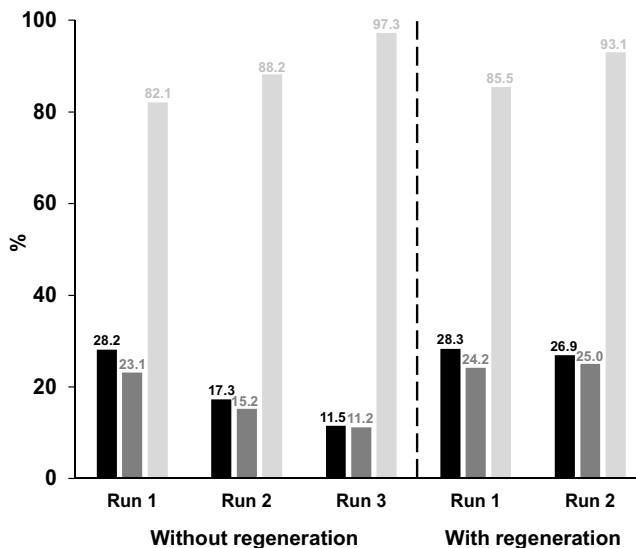


Fig. 6. Comparison of the glucose conversion (black), fructose yield (grey) and fructose selectivity (light grey) obtained for the 5%MgNaY zeolite after consecutive runs without and with regeneration of the catalyst, at 100 °C after 2 h.

product-catalyst suspension was collected and the catalyst was recovered by centrifugation. The catalyst was then washed with deionised water by centrifugation and used in the following run. Results are displayed in Fig. 6, where it can be seen that the activity of the sample decreases with the number of runs. As the amount of coke on the spent sample is not increasing with the number of runs (Table 4), deactivation observed in the second and third reaction runs could be mainly related to the Na and Mg leaching from the zeolite. Possibly, some degree of metal oxide particles agglomeration might also take place due to the presence of water in the reaction medium [54]. Moreover, this reduction of the glucose conversion is not linear with the number of catalytic tests, being more significant from the first to the second run. This observation is consistent with the sodium and magnesium leaching from the zeolite

after each run (Table 4), as the degree of cations leaching is much higher during the first run. Thus, the second run starts with a lower amount of Na and Mg on the catalyst than the first run, causing the decrease of activity. On the other hand, the quantity of sodium and magnesium on the catalyst in the beginning of second and third runs is similar, explaining the gradual stabilisation of the conversion. Moreau et al. [28] also verified a stabilisation of the activity of the catalyst after two consecutive runs, when carrying out glucose isomerisation over a NaX zeolite.

On the other hand, selectivity to fructose increases from 82.1 to 97.3% (glucose conversion from 28.2 to 11.5%) by performing consecutive runs (Fig. 6). Some possible reasons to explain this observation are: (i) carbonaceous deposits remaining after reaction in the zeolite pores block the stronger active sites responsible for the further conversion of fructose, (ii) the release of magnesium from the zeolite also reduces the number of active sites for fructose transformation (iii) possible sodium replacement by hydronium ions during leaching further decreases basicity of the sample reducing fructose decomposition and/or (iv) the partial removal of magnesium from the zeolite structure re-opens the pores of the sample, creating more space for the molecules diffusion, and so decreasing the probability of fructose subsequent transformation into other products. With the purpose of confirming or otherwise the latter hypothesis, nitrogen adsorption was carried out over the spent 5%MgNaY zeolite after the third reaction run (Table 1). It was found that after three runs both the microporous and mesoporous volumes of the zeolite have increased when compared to the fresh 5%MgNaY, which agrees with the partial released of magnesium from the zeolite and the re-opening of the pore structure. Besides, it could also be noticed that the external surface area of the reused sample also considerably increases, being even higher than the one for the pure NaY zeolite. Thus, it could be that magnesium removal causes a certain degree of erosion on the outer surface of the zeolite. However, the enhancement of the external surface area also contributes for the improvement of the molecules diffusion from the zeolite structure [59].

Interestingly, if after the first reaction a regeneration of the catalyst is carried out by heating the sample at 600 °C under air

Table 4

Sodium and magnesium leaching and coke retention on the catalyst for 5%MgNaY after consecutive runs without and with regeneration.

	Run	Na leaching% ^a (ppm) ^b	Na on catalyst (mg) ^c	Mg leaching% ^a (ppm) ^b	Mg on catalyst (mg) ^c	Coke (wt.%)
Without regeneration	First	27.9 (539)	9.65	7.2 (72)	5.00	3.6 ^d
	Second	7.3 (102)	6.95	1.3 (12)	4.64	-
	Third	4.8 (62)	6.44	1.5 (14)	4.58	2.7
With regeneration	First	28.2 (543)	9.65	7.8 (78)	5.00	3.6 ^d
	Second	8.0 (154)	6.93	7.8 (72)	4.61	2.3

^a Percentage of leaching calculated by dividing the amount of Na or Mg removed from the zeolite during the run to the amount of Na or Mg on the catalyst in the beginning of the run.

^b Concentration of Na or Mg in the liquid product (5 mL) after reaction.

^c Amount of Na or Mg on the catalyst in the beginning of the run.

^d Considered the same as for the single run presented in Table 2 for the 5%MgNaY due to impossibility of determination.

for 1 h, the zeolite sample is able to recover almost completely its initial activity when a second run is performed (Fig. 6), even though cations leaching has taken place (Table 4). Thus, it seems that carbonaceous materials accumulation on the zeolite also plays an important role in the catalyst deactivation. Nevertheless, higher amounts of sodium and magnesium are released from the zeolite during the second run with the regenerated catalyst (Table 4). This could be an indication that the calcination of the sample at high temperature causes some redistribution of the metals on the support [54], which can be expected to have a positive impact on the activity. It could also show that the presence of coke into the zeolite structure prevents to some extent the cations leaching phenomenon. The amount of magnesium lost after one reaction run is only about 0.4 mg of the initial 5 mg (Table 4). Regeneration via calcination at high temperature under oxidative medium (air) can cause redispersion of the remaining metal oxide particles, potentially decreasing their size leading to a recovery of the catalyst activity [54,60]. Formation of extra-framework aluminium species (Lewis acid sites) on the zeolite through calcination at high temperatures [61,62] could also lead to an increase of the activity [22,37–39]. To check this hypothesis, XRD was carried out for the spent sample after regeneration. The framework Si/Al ratio for the regenerated catalyst was calculated based on its unit cell parameter estimated from XRD (2.465 nm) using the Breck–Flanigen equation. A value of 2.6 was found for the spent regenerated sample, which is smaller than the framework Si/Al ratio for the NaY support (3.6) and matches its global Si/Al ratio. This indicates that no EFAL are being formed during the regeneration–calcination, but also that EFAL species are being leached from the zeolite during reaction.

Regarding fructose selectivity over the regenerated sample, an enhancement can be observed in comparison to the fresh catalyst, as well as in relation to the sample after the second run without regeneration (Fig. 6). Besides the possible causes for the increase of the selectivity previously mentioned, the elimination of the trapped carbon materials could also additionally re-open the pores, favouring the diffusion of the molecules inside the structure. This opening of the pores can be confirmed through the analysis given in Table 1. It can be seen that the regenerated sample has greater microporous and mesoporous volumes than the 5%MgNaY zeolite after 3 runs without regeneration, even if a lower amount of magnesium was removed from the former (78 ppm) when compared to the later (98 ppm), as shown in Table 4. Therefore, the higher enhancement of the textural properties for the regenerated sample can only be due to the carbonaceous material burn out from the zeolite structure.

Therefore, these results evidence that magnesium zeolite catalysts can successfully be used in consecutive reaction runs, particularly if an intermediate regeneration step is carried out since regeneration through calcination at high temperature under air re-activates the catalyst and further promotes fructose selectivity.

3.2.4. Performance of magnesium-impregnated zeolites vs. commonly used catalysts

Isomerisation of glucose to fructose was also performed over a commercial hydrotalcite (nominal Mg/Al = 3:1), a commercial magnesium oxide and a mechanical mixture 10 wt.% MgO + NaY, under identical conditions. Data found was compared to the results obtained for the prepared magnesium-zeolites catalysts (Fig. 7). Basic hydrotalcite containing 27 nominal-wt.% of magnesium in its structure presents after 2 h of reaction a glucose conversion of 34.4% and a fructose yield of 33.0% (fructose selectivity = 95.9%) indicating hydrotalcite is more selective to fructose than the zeolite-based catalysts. On the other hand, comparable fructose yields are achieved with hydrotalcites and the zeolites containing 10 and 15 wt.% of magnesium (32.4 and 31.9%, respectively). Furthermore, magnesium leaching was also found to take place on the hydrotalcite,

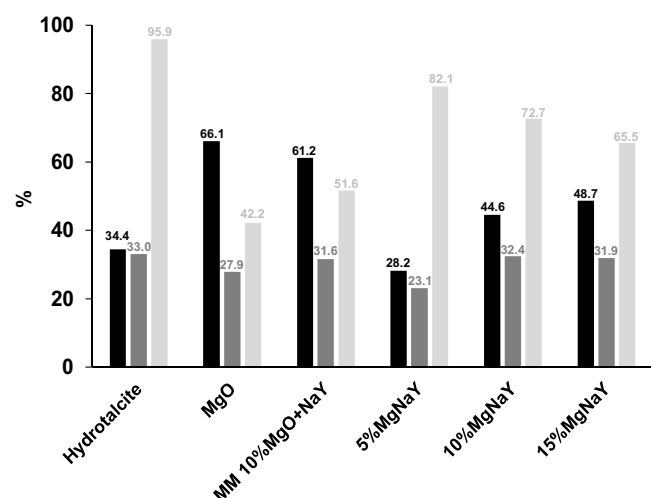


Fig. 7. Comparison of the glucose conversion (black), fructose yield (grey) and fructose selectivity (light grey) obtained for the commercial hydrotalcite, commercial MgO, 10 wt.% MgO + NaY zeolite mechanical mixture and the magnesium zeolites, at 100 °C after 2 h.

as 15% of the initial magnesium amount in the hydrotalcite was released to the liquid product during the reaction. Magnesium leaching from the hydrotalcites structure was also previously observed during glucose isomerisation to fructose by some authors [63,64], while other authors claim that no cation leaching occurs over hydrotalcites [28,29].

Regarding bulk magnesium oxide, this shows a much better activity than any of the other catalysts, reaching 66.1% of conversion (Fig. 7). This is even higher than the thermodynamic equilibrium conversion for glucose at the reaction conditions (57% [21]), which is explained by the significant formation of by-products through fructose decomposition displacing the equilibrium towards the products. For the level of conversion attained, fructose yield and selectivity are only 27.9 and 42.2% respectively. Similar results were found at identical operating conditions by Marianou et al. [35]. In fact, bulk magnesium oxide seems to have a much higher tendency to produce heavier compounds, as revealed by the high amount of coke found on the spent sample (47.8 wt.%), as well as by the strong dark brown colour of the reaction solution that indicates the presence of dehydration and condensation by-products [17]. This might signify that an extremely high basicity is not desirable for the production of fructose as it causes its further reaction and decomposition. When the bulk magnesium oxide is combined with the NaY in a mechanical mixture containing 10 wt.% of the former, glucose conversion decreases to 61.2%, but an improvement in the fructose yield (31.6%) is noticed, and therefore in the corresponding selectivity (51.6%). This could show that a decrease in the overall basicity might avoid additional fructose transformation.

For comparison purposes, deactivation was analysed for the commercial hydrotalcite and bulk MgO by performing two consecutive reaction cycles without intermediate regeneration, similar to the study of 5%MgNaY zeolite (Fig. 6). All the catalysts lose activity in the second run: from 34.0 to 15.2% and from 66.6 to 58.4% for the commercial hydrotalcite and bulk MgO respectively. Therefore, the deactivation degree follows the order: hydrotalcite > zeolite > MgO. Concerning fructose yield, while a decrease occurs for the hydrotalcite (33.6 to 15.4%), MgO shows similar fructose yields in both runs (32.0 and 35.6%). However, the amount of glucose required to achieve these fructose yields is always very high for MgO compared to hydrotalcites or the Mg-impregnated zeolites.

Finally, the performances of the best prepared zeolites in the present work were compared to those of the catalysts previously reported in the literature for the glucose isomerisation into fruc-

Table 5 Comparison of the performance of different studied heterogeneous catalysts for the glucose isomerisation into fructose.

Catalyst	Temp. (°C)	Time (h)	Catalyst amount (g)	Glucose conversion (%)	Glucose consumption (g glucose/g catalyst/h)	Fructose yield (%)	Fructose productivity (g fructose/g catalyst/h)	Fructose selectivity (%)	Ref.
NaA	95	1	1	26	0.87	19	0.62	72	[28]
CSA	95	1	1	34	1.13	22	0.75	66	
NaX	95	1	1	20	0.67	17	0.57	86	
CSX	95	1	1	25	0.83	19	0.64	77	
NaY	95	1	1	9	0.30	6	0.19	62	
CSY	95	1	1	10	0.33	6	0.21	63	
Hydroalumite (Mg/Al = 2.5)	95	1	1	30	1.00	20	0.66	66	
Hydroalumite (Mg/Al = 3)	95	1	1	42	1.40	25	0.84	60	
Mg _{0.74} Al _{0.26} (OH) ₂ (CO ₃) _{0.13} ·0.91H ₂ O	110	1.5	0.1	30	1.10	26	0.95	85	[64]
Ti-BEA	140	1.5	—	—	—	23	—	45	[22]
Ti-MCM-41	140	1.5	—	23	—	7	—	30	
Sr-BEA	140	1.5	—	80	—	24	—	30	
Sr-MCM-41	140	1.5	—	30	—	12	—	40	
Sr-BEA	110	0.5	—	55	—	32	—	58	
Na ₉ Si ₁₂ Ti ₅ O ₃₈ (OH)	100	2	0.02	48	0.60	39	0.49	84	[36]
Na ₃ (NaH)Si ₂ O ₂ [Si ₂ O ₆] ₂	100	2	0.02	56	0.70	34	0.43	62	
HfCa ₂ Si ₈ O ₁₉	100	2	0.02	54	0.68	34	0.43	64	
Ca ₅ Si ₆ O ₁₇	100	2	0.02	51	0.64	35	0.44	69	
[CTA]Si-MCM-48	100	2	—	3	—	2	—	50	
[CTA]Si-MCM-50	100	2	—	16	—	14	—	88	
[CTA]Si-MCM-41	100	2	—	21	—	17	—	81	
SiO ₂ /Al ₂ O ₃	100	1	—	1	0.17	1	0.03	17	
MgO	90	0.75	0.25	44	1.34	26	0.51	38	
10%MgNaY	100	2	0.1	45	4.70	33	3.56	76	
10%MgNaY	100	0.5	0.1	35	3.50	32	0.81	73	
15%MgNaY	100	2	0.1	49	1.22	32	0.80	87	
								66	Present study

tose, in order to truly validate whether they are suitable catalysts for this reaction. This comparison was based on the analysis of glucose conversion and consumption, as well as fructose yield, productivity and selectivity, for all the catalysts (Table 5). Overall, it can be seen that the zeolites from this study show similar or superior fructose productivity when compared to the other catalysts, even when the best result for MgO is considered. This confirms that Mg-impregnated NaY catalysts could be considered for glucose isomerisation into fructose, especially taking into account that NaY zeolite is a commercially available support and magnesium incorporation is an easy process. However, a techno-economic and life cycle analysis would be desirable to establish the utility of these catalysts.

4. Conclusion

Glucose isomerisation into fructose was carried out in aqueous medium at 100 °C over Mg-impregnated NaY zeolite catalysts. Despite a slight decrease in crystallinity and reduction of the textural properties of the zeolites due to magnesium addition, magnesium-based NaY zeolites revealed improved performances for glucose isomerisation into fructose as a result of the increased number of basic sites. While glucose conversion increases after 2 h of reaction from about 6–49% by magnesium addition (0–15 wt.%), there is a decrease in fructose selectivity from 96 to 66%. The fructose yields for the samples containing 10 and 15 wt.% of magnesium are comparable to that obtained with a commercial hydroalumite (nominal Mg/Al = 3) and higher than found for pure magnesium oxide. The main causes of catalyst deactivation were identified to be carbonaceous materials accumulation on the zeolites and cations leaching from the zeolite structure.

Deactivation was studied further by performing consecutive reaction tests. In absence of any catalyst regeneration, zeolites lose their activity in subsequent runs mainly due to cations leaching from the zeolite structure to the liquid, where this effect is gradually attenuated with the number of runs. However, if an intermediate regeneration is done, the samples are capable of almost completely recovering their initial activity, due to coke combustion and cations redistribution. In both cases selectivity to fructose is improved compared to the fresh catalyst as a result of re-opening of the zeolite pores due to cations leaching and/or carbon removal. Cations leaching leads to the occurrence of a parallel homogeneous reaction. The heterogeneous catalytic contribution remains the more significant, except for the highly loaded 15 wt.% Mg zeolite.

Hence, magnesium-impregnated NaY zeolites have been demonstrated to be very promising catalysts for the glucose isomerisation into fructose, presenting glucose consumption rates and fructose productivities similar or higher than the various catalysts already reported in the literature. In addition, the catalysts have potential to be recycled and reused, as they exhibit good stability after consecutive reaction tests if an intermediate regeneration is carried out.

Acknowledgement

This work was performed with financial support from EPSRC(UK) under grant EP/K014749/1.

Appendix A. Supplementary data

Supplementary data associated with this article can be found, in the online version, at <http://dx.doi.org/10.1016/j.apcatb.2017.01.037>.

References

- [1] G.W. Huber, S. Iborra, A. Corma, Synthesis of transportation fuels from biomass: chemistry, catalysts, and engineering, *Chem. Rev.* 106 (2006) 4044–4098.
- [2] V. Menon, M. Rao, Trends in bioconversion of lignocellulose: biofuels platform chemicals & biorefinery concept, *Prog. Energy Combust. Sci.* 38 (2012) 522–550.
- [3] S.K. Maity, Opportunities, recent trends and challenges of integrated biorefinery: part I, *Renew. Sustain. Energy Rev.* 43 (2015) 1427–1445.
- [4] S. Octave, D. Thomas, Biorefinery: toward an industrial metabolism, *Biochimie* 91 (2009) 659–664.
- [5] J.-P. Lange, Lignocellulose conversion: an introduction to chemistry, process and economics, *Biofuels Bioprod. Bioref.* 1 (2007) 39–48.
- [6] J.C. Escobar, E.S. Lora, O.J. Venturini, E.E. Yáñez, E.F. Castillo, O. Almazam, Biofuels: environment, technology and food security, *Renew. Sustain. Energy Rev.* 13 (2009) 1275–1287.
- [7] D. Mohan, C.U. Pittman Jr., P.H. Steele, Pyrolysis of wood/biomass for bio-oil: a critical review, *Energy Fuels* 20 (2006) 848–889.
- [8] F. Carvalheiro, L. Duarte, F.M. Gírio, Hemicellulose biorefineries: a review on biomass pretreatments, *J. Sci. Ind. Res.* 67 (2008) 849–864.
- [9] Use of Sugars and Other Carbohydrates in the Food Industry, vol. 12, American Chemical Society, 1955.
- [10] P. Hull, Glucose Syrups: Technology and Applications, first edition, Wiley-Blackwell, United Kingdom, 2010.
- [11] H.G. Garg, M.K. Cowman, C.A. Hales, Carbohydrate Chemistry, Biology and Medical Applications, first edition, Elsevier, Oxford, 2008.
- [12] M. Aresta, A. Dibenedetto, F. Dumeignil, Biorefinery: Biomass to Chemicals and Fuels, De Gruyter, Germany, 2012.
- [13] Bio-based Chemicals: Value Added Products from Biorefineries, IEA Bioenergy, 2012.
- [14] J.N. Chheda, G.W. Huber, J.A. Dumesic, Liquid-phase catalytic processing of biomass-derived oxygenated hydrocarbons to fuels and chemicals, *Angew. Chem. Int. Ed.* 46 (2007) 7164–7183.
- [15] X. Qian, Mechanisms and energetics for Brønsted acid-catalyzed glucose condensation, dehydration and isomerization reactions, *Top. Catal.* 55 (2012) 218–226.
- [16] R.-J. van Putten, J.C. van der Waal, E. de Jong, C.B. Rasrendra, H.J. Heeres, J.G. de Vries, Hydroxymethylfurfural, a versatile platform chemical made from renewable resources, *Chem. Rev.* 113 (2013) 1499–1597.
- [17] I. Delidovich, R. Palkovits, Catalytic isomerization of biomass-derived aldoses: a review, *ChemSusChem* 9 (2016) 547–561.
- [18] T. Buntara, S. Noel, P.H. Phua, I. Melián-Cabrera, J.G. de Vries, H.J. Heeres, Caprolactam from renewable resources: catalytic conversion of 5-hydroxymethylfurfural into caprolactone, *Angew. Chem. Int. Ed.* 50 (2011) 7083–7087.
- [19] V.J. Jensen, S. Rugh, Industrial-scale production and application of immobilized glucose isomerase, *Methods Enzymol.* 136 (1987) 356–370.
- [20] K. Buchholz, J. Seibel, Industrial carbohydrate biotransformations, *Carbohydr. Res.* 343 (2008) 1966–1979.
- [21] Y.B. Tewari, R.N. Goldberg, Thermodynamics of the conversion of aqueous glucose to fructose, *J. Solut. Chem.* 13 (1984) 523–547.
- [22] M. Moliner, Y. Román-Leshkov, M.E. Davis, Tin-containing zeolites are highly active catalysts for the isomerization of glucose in water, *PNAS* 107 (2010) 6164–6168.
- [23] G. de Wit, A.P.G. Kieboom, H. van Bekkum, Enolisation and isomerisation of monosaccharides in aqueous, alkaline solution, *Carbohydr. Res.* 74 (1979) 157–175.
- [24] S.J. Angyal, Glycoscience, vol. 15, Springer, Berlin, 2001, pp. 1–14.
- [25] J.M. Carraher, C.N. Fleitman, J.-P. Tessonner, Kinetic and mechanistic study of glucose isomerization using homogeneous organic Brønsted base catalysts in water, *ACS Catal.* 5 (2015) 3162–3173.
- [26] C. Liu, J.M. Carraher, J.L. Swedberg, C.R. Herndon, C.N. Fleitman, J.-P. Tessonner, Selective base-catalyzed isomerization of glucose to fructose, *ACS Catal.* 4 (2014) 4295–4298.
- [27] V. Choudhary, A.B. Pinar, R.F. Lobo, D.G. Vlachos, S.I. Sandler, Comparison of homogeneous and heterogeneous catalysts for glucose-to-fructose isomerization in aqueous media, *ChemSusChem* 6 (2013) 2369–2376.
- [28] C. Moreau, R. Durand, A. Roux, D. Tichit, Isomerization of glucose into fructose in the presence of cation-exchanged zeolites and hydrotalcites, *Appl. Catal. A: Gen.* 193 (2000) 257–264.
- [29] J. Lecomte, A. Finiels, C. Moreau, Kinetic study of the isomerization of glucose into fructose in the presence of anion-modified hydrotalcites, *Starch/Stärke* 54 (2002) 75–79.
- [30] C. Moreau, J. Lecomte, A. Roux, Determination of the basic strength of solid catalysts in water by means of a kinetic tracer, *Catal. Commun.* 7 (2006) 941–944.
- [31] S. Yu, E. Kim, S. Park, I.K. Song, J.C. Jung, Isomerization of glucose into fructose over Mg-Al hydrotalcite catalysts, *Catal. Commun.* 29 (2012) 63–67.
- [32] R. Shukla, X.E. Verykios, R. Mijtharasan, Isomerization and hydrolysis reactions of important disaccharides over inorganic heterogeneous catalysts, *Carbohydr. Res.* 143 (1985) 97–106.
- [33] L. Lv, X. Guo, P. Bai, S. Zhao, Isomerization of glucose into fructose and mannose in presence of anion-exchanged resins, *Asian J. Chem.* 27 (2015) 2774–2778.
- [34] R.O.L. Souza, D.P. Fabiano, C. Feche, F. Rataboul, D. Cardoso, N. Essayem, Glucose–fructose isomerisation promoted by basic hybrid catalysts, *Catal. Today* 195 (2012) 114–119.
- [35] A.A. Marianou, C.M. Michalof, A. Pineda, E.F. Iliopoulos, K.S. Triantafyllidis, A.A. Lappas, Glucose to fructose isomerization in aqueous media over homogeneous and heterogeneous catalysts, *ChemCatChem* 8 (2016) 1100–1110.
- [36] S. Lima, A.S. Dias, Z. Lin, P. Brandão, P. Ferreira, M. Pillinger, J. Rocha, V. Calvino-Casilda, A.A. Valente, Isomerization of d-glucose to d-fructose over metallosilicate solid bases, *Appl. Catal. A: Gen.* 339 (2008) 21–27.
- [37] G. Li, E.A. Pidko, E.J.M. Hensen, Synergy between Lewis acid sites and hydroxyl groups for the isomerization of glucose to fructose over Sn-containing zeolites: a theoretical perspective, *Catal. Sci. Technol.* 4 (2014) 2241–2250.
- [38] N. Rajabbeigi, A.I. Torres, C.M. Lew, B. Elyassi, L. Ren, Z. Wang, H.J. Cho, W. Fan, P. Daoutidis, M. Tsapatsis, On the kinetics of the isomerization of glucose to fructose using Sn-Beta, *Chem. Eng. Sci.* 116 (2014) 235–242.
- [39] S. Saravananurugan, M. Paniagua, J.A. Melero, A. Riisager, Efficient isomerization of glucose to fructose over zeolites in consecutive reactions in alcohol and aqueous media, *J. Am. Chem. Soc.* 135 (2013) 5246–5249.
- [40] R. Netrabukkana, K. Lourvanij, G.L. Rorrer, Diffusion of glucose and glucitol in microporous and mesoporous silicate/aluminosilicate catalysts, *Ind. Eng. Chem. Res.* 35 (1996) 458–464.
- [41] A. Corma, S. Iborra, Optimization of alkaline earth metal oxide and hydroxide catalysts for base-catalyzed reactions, *Adv. Catal.* 49 (2006) 239–302.
- [42] M.M.J. Treacy, J.H. Higgins, Collection of Simulated XRD Powder Patterns for Zeolites, Elsevier, 2001.
- [43] M.A. Aramendía, J.A. Benítez, V. Borau, C. Jiménez, J.M. Marinas, J.R. Ruiz, F. Urbano, Characterization of various magnesium oxides by XRD and ^{1}H MAS NMR spectroscopy, *J. Solid State Chem.* 144 (2009) 25–29.
- [44] A.A. Rownaghi, R.L. Huhnke, Producing hydrogen-rich gases by steam reforming of syngas tar over CaO/MgO/NiO catalysts, *ACS Sustain. Chem. Eng.* 1 (2013) 80–86.
- [45] M. Laspéras, H. Cambon, D. Brunel, I. Rodriguez, P. Geneste, Characterization of basicity in alkaline cesium-exchanged X zeolites post-synthetically modified by impregnation: a TPD study using carbon dioxide as a probe molecule, *Microporous Mater.* 1 (1993) 343–351.
- [46] K. Noiroj, P. Intarapong, A. Luengnaruemitchai, S. Jai-In, A comparative study of KOH/Al₂O₃ and KOH/NaY catalysts for biodiesel production via transesterification from palm oil, *Renew. Energy* 34 (2009) 1145–1150.
- [47] N. Supamathanon, J. Wittayakun, S. Prayoonpokarach, W. Supronowicz, F. Roessner, Basic properties of potassium oxide supported on zeolite y studied by pyrrole-tpd and catalytic conversion of methylbutynol, *Quim. Nova* 35 (2012) 1719–1723.
- [48] H.Y. Kim, H.M. Lee, J.-N. Park, Bifunctional mechanism of CO₂ methanation on Pd-MgO/SiO₂ catalyst: independent roles of MgO and Pd on CO₂ methanation, *J. Phys. Chem. C* 114 (2010) 7128–7131.
- [49] J.I. Di Cosimo, V.K. Díez, M. Xu, E. Iglesias, C.R. Apesteguía, Structure and surface and catalytic properties of Mg-Al basic oxides, *J. Catal.* 178 (1998) 499–510.
- [50] T. Belin, C. Mve Mfoumou, S. Mignard, Y. Pouilloux, Study of physisorbed carbon dioxide on zeolites modified by addition of oxides or acetate impregnation, *Microporous Mesoporous Mater.* 182 (2013) 109–116.
- [51] J.I. Di Cosimo, V.K. Díez, C. Ferretti, C.R. Apesteguía, Basic catalysis on MgO: generation, characterization and catalytic properties of active sites, *Catalysis* 26 (2014) 1–28.
- [52] E.G. Derouane, Catalysis for Fine Chemical Synthesis, Micro and Mesoporous Solid Catalysts, vol. 4, John Wiley & Sons Ltd, England, 2006.
- [53] M.A.B. Siddiqui, A.M. Aitani, M.R. Saeed, N. Al-Yassir, S. Al-Khattaf, Enhancing propylene production from catalytic cracking of Arabian Light VGO over novel zeolites as FCC catalyst additives, *Fuel* 90 (2011) 459–466.
- [54] M. Guisnet, F. Ramôa Ribeiro, Deactivation and Regeneration of Zeolite Catalysts, Imperial College Press, 2011.
- [55] Y. Ye, Q. Liu, J. Wang, Influence of saccharides chelating agent on particle size and magnetic properties of Co₂Z hexaferrite synthesized by sol-gel method, *J. Sol-Gel Sci. Technol.* 60 (2011) 41–47.
- [56] K.R. Franklin, R.P. Townsend, S.J. Whelan, C.J. Adams, Ternary exchange equilibria involving H₃O⁺, NH₄⁺ and Na⁺ ions in synthetic zeolites of the faujasite structure, *Stud. Surf. Sci. Catal.* 28 (1986) 289–296.
- [57] R.P. Townsend, Ion exchange in zeolites: some recent developments in theory and practice, *Pure Appl. Chem.* 58 (1986) 1359–1366.
- [58] H.G. Karge, J. Weitkamp, Post-Synthesis Modifications I, Springer, Germany, 2002.
- [59] I. Graça, A.M. Carmo, J.M. Lopes, M.F. Ribeiro, Improving HZSM-5 resistance to phenolic compounds for the bio-oils/FCC feedstocks co-processing, *Fuel* 140 (2015) 484–494.
- [60] K. Morgan, A. Goguet, C. Hardacre, Metal redispersion strategies for recycling of supported metal catalysts: a perspective, *ACS Catal.* 5 (2015) 3430–3445.
- [61] M. Guisnet, J.-P. Gilson, Zeolites for Cleaner Technologies, Imperial College Press, London, 2002.
- [62] A. Corma, Inorganic solid acids and their use in acid-catalyzed hydrocarbon reactions, *Chem. Rev.* 95 (1995) 559–614.
- [63] I. Delidovich, R. Palkovits, Catalytic activity and stability of hydrophobic Mg-Al hydrotalcites in the continuous aqueous-phase isomerization of glucose into fructose, *Catal. Sci. Technol.* 4 (2014) 4322–4329.
- [64] I. Delidovich, R. Palkovits, Structure–performance correlations of Mg-Al hydrotalcite catalysts for the isomerization of glucose into fructose, *J. Catal.* 327 (2015) 1–9.